



Preliminary study of the response of the CALICE tungsten tile HCAL prototype to electrons and pions.

Piotr Rymaszewski, AGH University of Science and Technology, Poland

Supervisor: Shaojun Lu

September 9, 2011

Abstract

First chapter contains short description of HCAL and it's working principles. Next part shows main focus of project - data from working prototype is analysed, data cuts are introduced and explained, response to electrons and pions is studied and as result linearity and resolution of HCAL are obtained. Third chapter includes short analysis of temperature influence on HCAL. In chapter four summary of obtained results is presented.

Contents

1	Introduction - brief description of HCAL	3
2	Analysis of data from physical prototype of HCAL	5
2.1	Obtained data	5
2.2	Data cuts	5
2.2.1	Cherenkov threshold detector	5
2.2.2	Shower shape	7
2.2.2.1	Electrons	7
2.2.2.2	Muons	9
2.3	Results of data cuts	9
2.4	Linearity of response & resolution for electron beam	13
2.5	Linearity of response & resolution for pion beam	15
2.6	Temperature influence on work of detector's prototype	17
2.6.1	Influence of temperature on value of reconstructed energy	18
2.6.2	Temperature profile	18
3	Summary	20

1 Introduction - brief description of HCAL

International Linear Collider (ILC) is one of proposed "successors" of LHC - it would be supposed to carry out precise measurements of Higgs boson if LHC will prove it's existence. ILC is planned as e^+e^- collider with collision energy up to $1,5\text{ GeV}$.

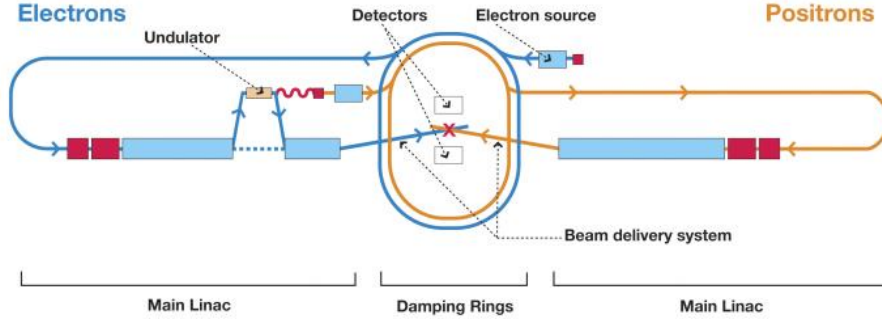
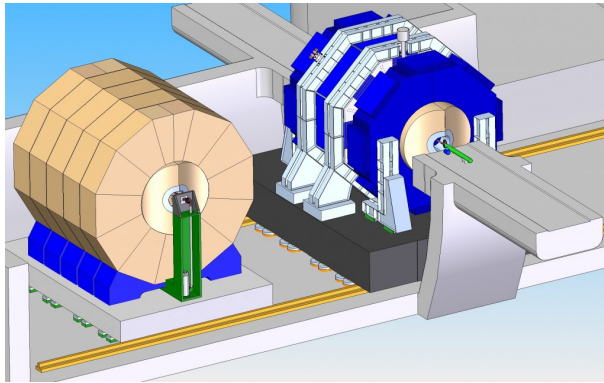
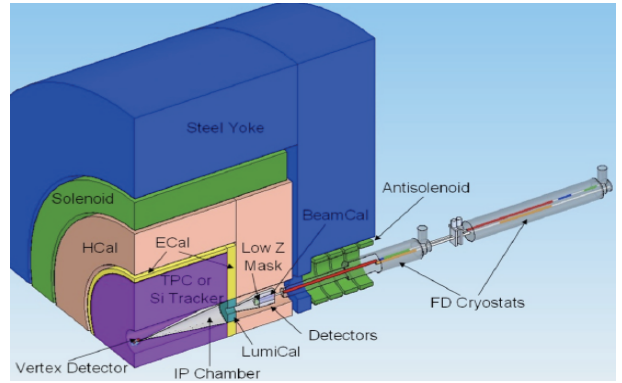


Figure 1: ILC schematic

As can be seen from figure 1 ILC will have two detectors: International Large Detector (ILD) and Silicon Detector (SiD). Handronic calorimeter (HCAL), from which prototype data has been analysed by me during this summer student programme, is part of of ILD (as shown in figure 2).



ILD (left) and SiPM (right)



Section of ILD showing HCAL placement

Figure 2: ILC detectors.

HCAL is a sampling calorimeter, which means that it is build out of alternating layers of absorber (10 mm thick tungsten) and active layers (5 mm plastic scintillator). In year 2010 prototype was build out of 30 layers, in 2011 eight more were added.

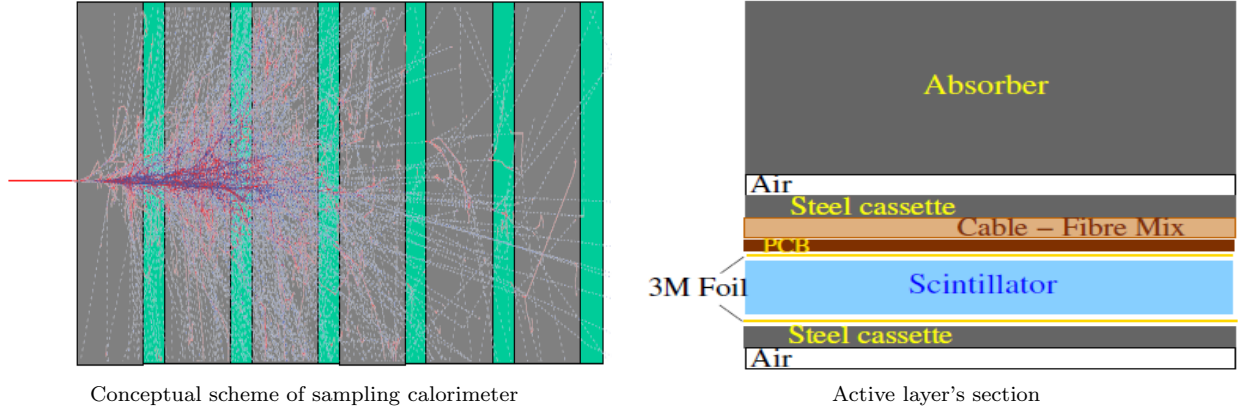


Figure 3: Sampling calorimeter

One of the most important features of HCAL is it's high granularity - active layer is build out of small tiles, varying in size: $3 \times 3 \text{ cm}$, $6 \times 6 \text{ cm}$ and $12 \times 12 \text{ cm}$ (layout of tiles is shown in figure 4). Such construction of active layer allows for better, more accurate measurements (e.g. ones can more precisely say where the beam hit detector and see more clearly how particle shower behaved). In figure 5 photographs of parts of active layers are shown. Working principle of this device is, putting it simply, as follows: light produced by plastic scintillator is capture by optic fibre, which transfers it to silicon photomultipliers (attached at both ends of fibre). Depending on amount of photons hitting SiPM (which contain 1156 pixels) different amplitude of signal is obtained.

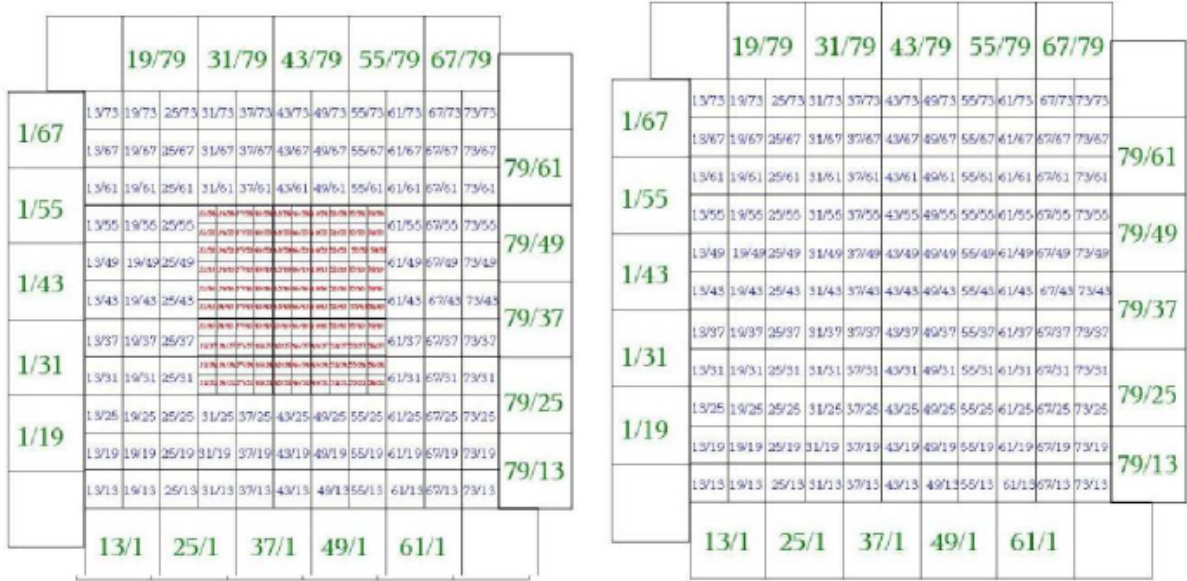
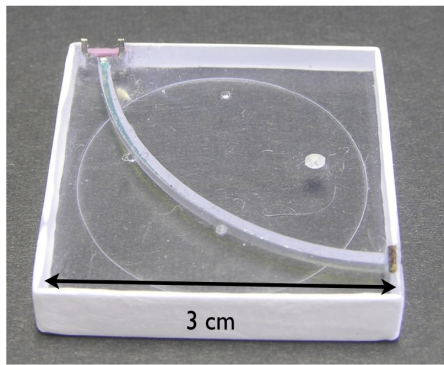
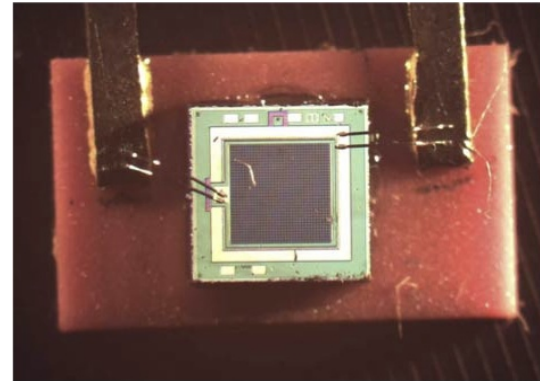


Figure 4: Active layer - high granularity grid layout (on the left 1st – 30th layer, on the right 31st – 38th layer)



Single tile



Silicon photomultiplier (SiPM)

Figure 5: Parts of active layer

2 Analysis of data from physical prototype of HCAL

2.1 Obtained data

To obtain ROOT files with which I have worked, I needed to produce steering files and use CALICE software. Output files were large ROOT trees, containing many information from each run (by "run" I mean test of detector with beam of specified particles with specified energy, one ROOT tree contained information only from one run). Information that is needed to describe detector performance is it's response to different beams (differing by particles and energies). When one have such information, than qualities like linearity or resolution can be computed, but finding real energy response is not so easy. Main difficulty is impurity of beam - although it is supposed to be beam of particles of just one kind, this is never the case. Data I have worked with was obtained during tests with two kinds of beams: electron and pion (in both cases tests with positively and negatively charged particles were carried out), but analysis shows that in reality in all runs detector was subjected to beam of mixed particle content - muons and pions were always present (even in electron beam runs), occasionally kaons could be observed. Such situation is nothing unusual, but as a result first step of finding detector's prototype behaviour is finding the real response to particular particles, which is done by cleaning up data. To do this data cuts were used.

2.2 Data cuts

In this section used data cuts will be presented and explained.

2.2.1 Cherenkov threshold detector

As stated in chapter 2.1 beam impurity is expected and as result some additional hardware is installed at test beam facility to make separation easier. One of such devices, used during testing of HCAL prototype, is Cherenkov threshold detector. It is relatively simple devices (schematic is presented in figure 6) - tube filled with gas, with mirror

and photomultiplier inside. If a fast moving particle enters tube cone of light can be produced (this happens if particle is moving faster than light in gas filling the tube). If this occurs light is reflected by mirror to photomultiplier, thus signal is produced.

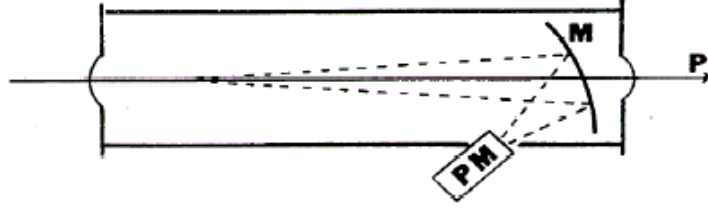


Figure 6: Simple schematic of Cherenkov threshold detector

Value of threshold momentum p_t for particle of mas m is given by (n_0 is refractive index under atmospheric pressure P_0):

$$p_t = \frac{mc}{\sqrt{\left[(n_0 - 1)\frac{P}{P_0} + 1\right]^2 - 1}} \quad (1)$$

Table 1: Table containing threshold pressures $P[atm]$ for particles of given type and momentum

Momentum [GeV]	Electron	Muon	Pion
1	0,0004	13,23	23,02
2	0,0001	3,31	5,78
3	0	1,47	2,57
4	0	0,83	1,45
5	0	0,53	0,93
6	0	0,37	0,64
7	0	0,27	0,47
8	0	0,21	0,36
9	0	0,16	0,29
10	0	0,13	0,23

Two of such devices are installed in front of HCAL prototype at test beam facility, so if pressures are set up correctly (according to table 1) separation of events caused be different particles during run is possible (ROOT tree containing run data has branches called "cherenkovBit" and "cherenkov2Bit" - if specific Cherenkov detectors was triggered for an event, bit 1 is assigned, if it has not triggered bit 0). In figure 7 two dimensional histogram is presented showing distribution of Cherenkov detectors trigger bits and each bits combination is marked with appropriate particles.

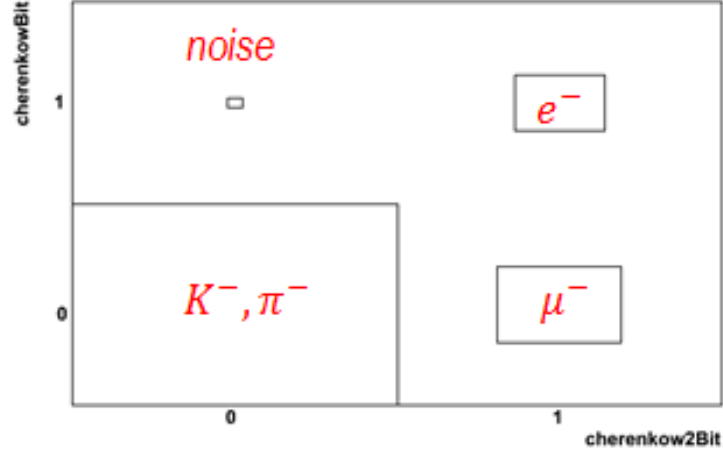


Figure 7: Two dimensional histogram showing distribution of detectors trigger bits for $4\text{GeV } e^-$ run with $0,6\text{atm}$ in 1st detector and $1,25\text{atm}$ in 2nd.

Main disadvantage of this method is it's applicability range - threshold pressures table is given only to 10GeV . Also separation is not very good when pressures of gas inside detectors are close to threshold pressures.

2.2.2 Shower shape

Second kind of data cuts is based on shape and properties of shower created by particles interacting with detector's matter. As we know different kinds of particles create different shower (simple visualisation is shown in figure 8)

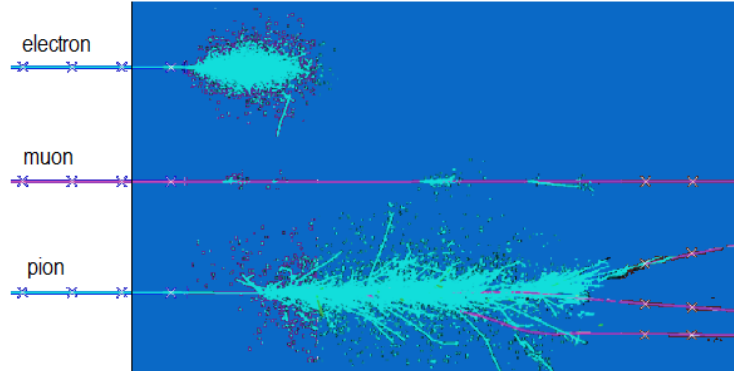


Figure 8: Shower shapes of different particles when interacting with matter.

2.2.2.1 Electrons

As can be seen in figure 8 shower created by electron is rather shallow - great majority of energy is deposited in first few layers of detector. This observation is in agreement

with plot shown in figure 9, which was obtained from Monte Carlo generated data (using *QGSP_BERT* model).

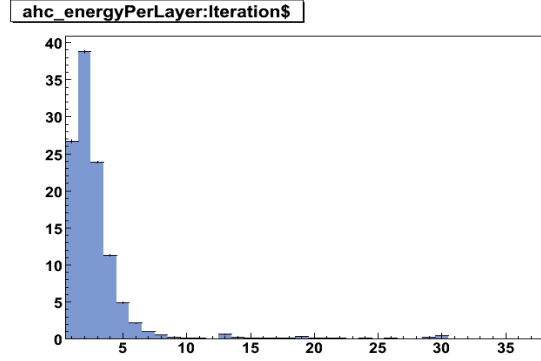


Figure 9: Distribution of mean energy values in detector's layers for $4\text{GeV } e^-$ MC generated run.

Introducing new variable η , which describes what fraction of energy is deposited in first M layer ($E(i)$ is energy deposited in i -th layer, N is total number of layers varying depending on year in which test has been made: for 2010 $N = 30$, for 2011 $N = 38$):

$$\eta = \frac{\sum_{m=1}^M E(m)}{\sum_{n=1}^N E(n)} \quad (2)$$

If $N = 5$ is chosen (based on plot in figure 9) and value of η is plotted, for MC generated (100% pure) data one can expect values near to one (figure 10 on the left), so when the same variable is plotted for real test beam data (figure 10 on the right) one can assume that events with $\eta > 0,8$ are due to interaction with electrons (it can be clearly seen, that using just this cut is not enough to get high purity data).

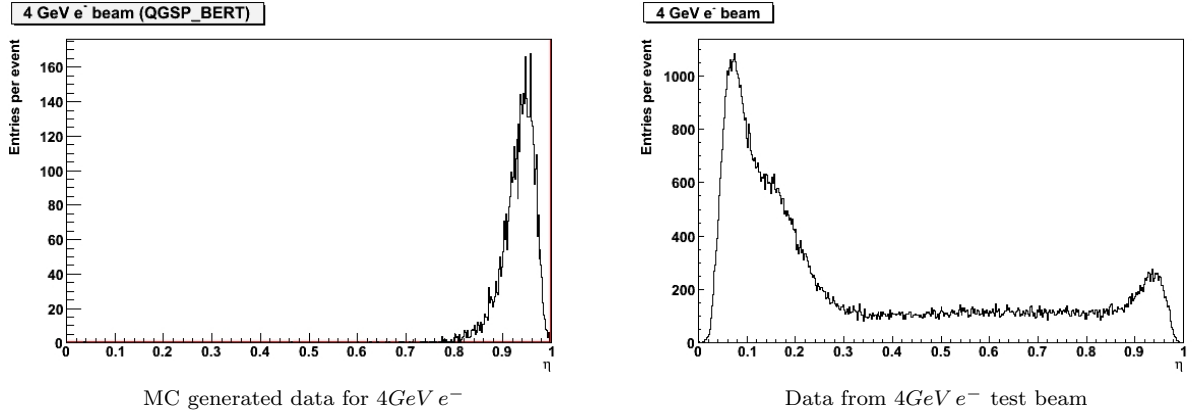


Figure 10: η value plots

2.2.2.2 Muons

As figure 8 shows muons pass through matter without producing any showers and depositing low amounts of energy. It can be observed e.g. by looking at the left part of figure 11, which shows energy distribution from Monte Carlo generated data for e^- and μ^- - muons can be observed only in low energy end of scale. This fact can be used to make selection, e.g. as shown at the right part of figure 11 which shows energy distribution for $4\text{GeV } e^-$ after applying cut provided by Cherenkov threshold detectors - muon events were marked with red circle.

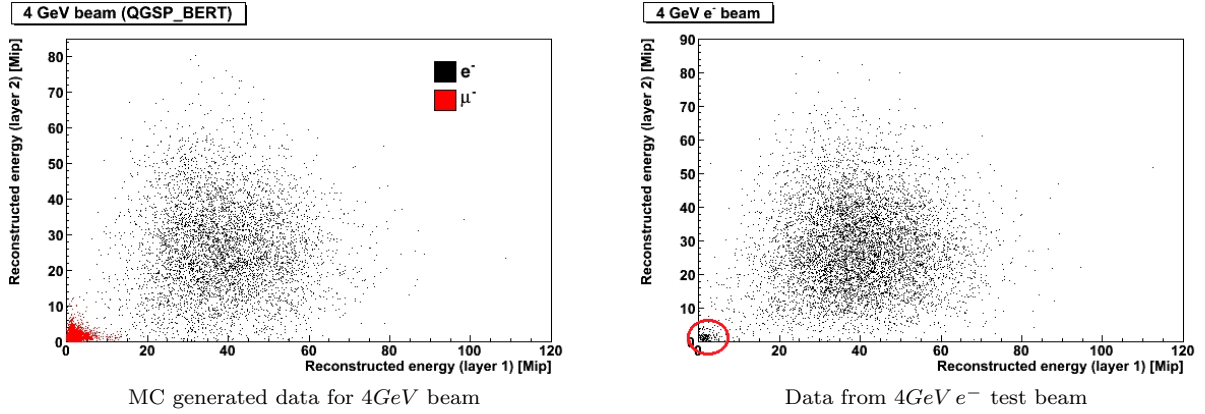


Figure 11: Two dimensional histograms presenting energy distribution in 1st and 2nd layer

Another method of making cut on muon events is using number of hits produced by event in layer - for muons low (1 or 2) hits per layer are expected.

2.3 Results of data cuts

To better illustrate necessity of making data cuts in figure 12 comparison of reconstructed energy distribution before and after applying cuts - in this particular case most of events are discarded (it is not always such large fraction but, as demonstrated, it can happen). Figures 13 - 17 present data after cuts, showing detector's prototype response to different kinds of beam (black lines are Gaussian fits).

Figure 17 shows that HCAL's prototype in current configuration cannot contain whole shower caused by π^- of energy above 150GeV - it shows in plot as tail on the left side of energy distribution.

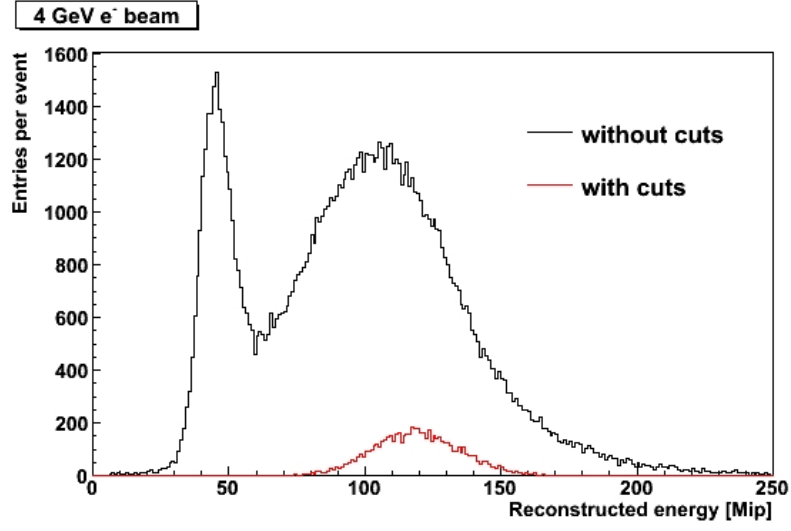


Figure 12: Comparison of reconstructed energy distribution before and after applying data cuts for $4\text{GeV } e^-$ run.

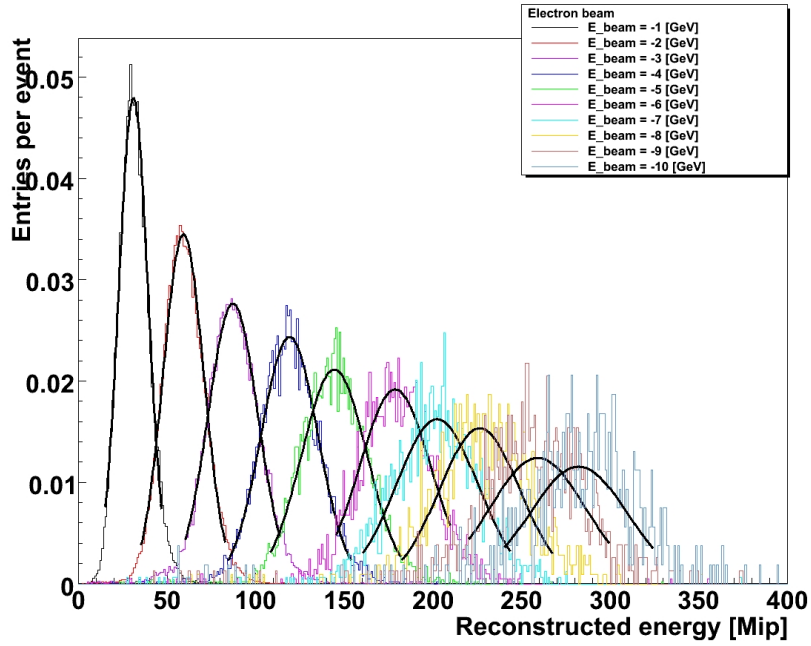


Figure 13: Energy response to e^- beam.

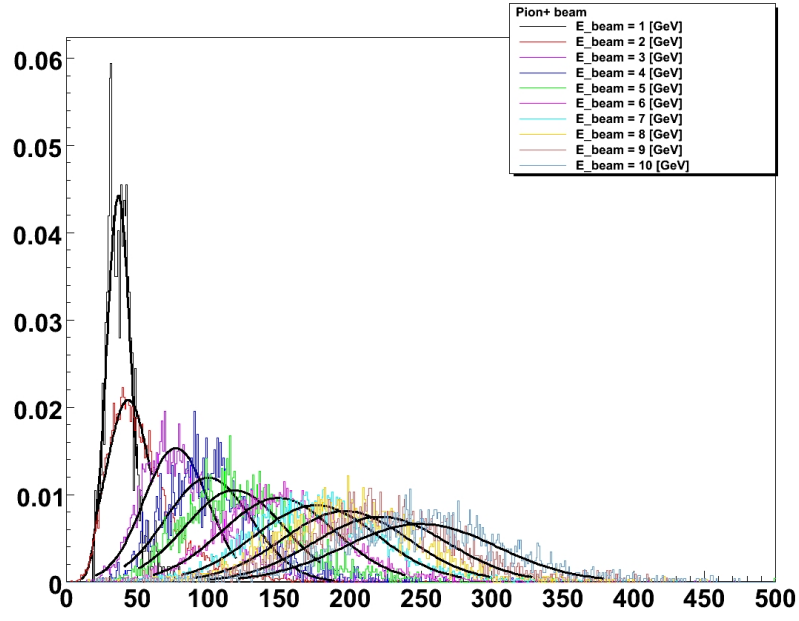


Figure 14: Energy response to π^+ beam.

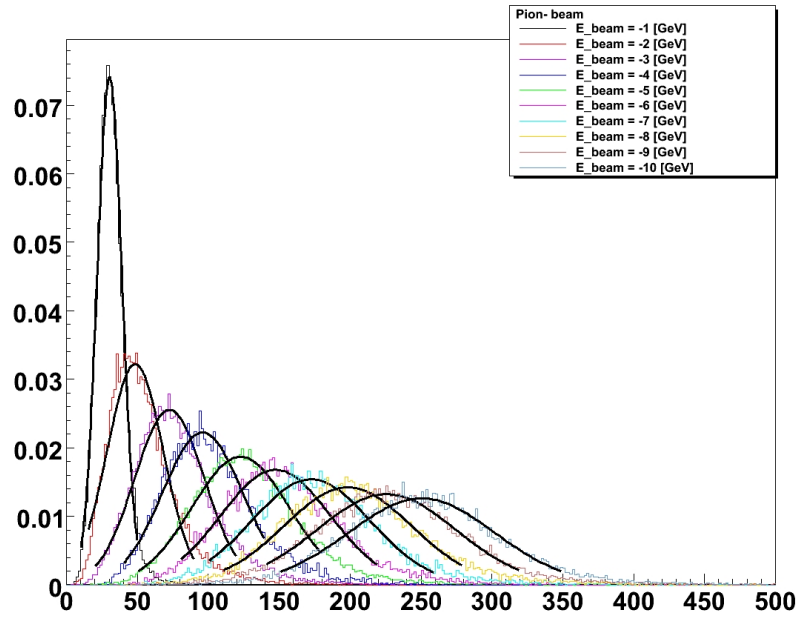


Figure 15: Energy response to π^- beam.

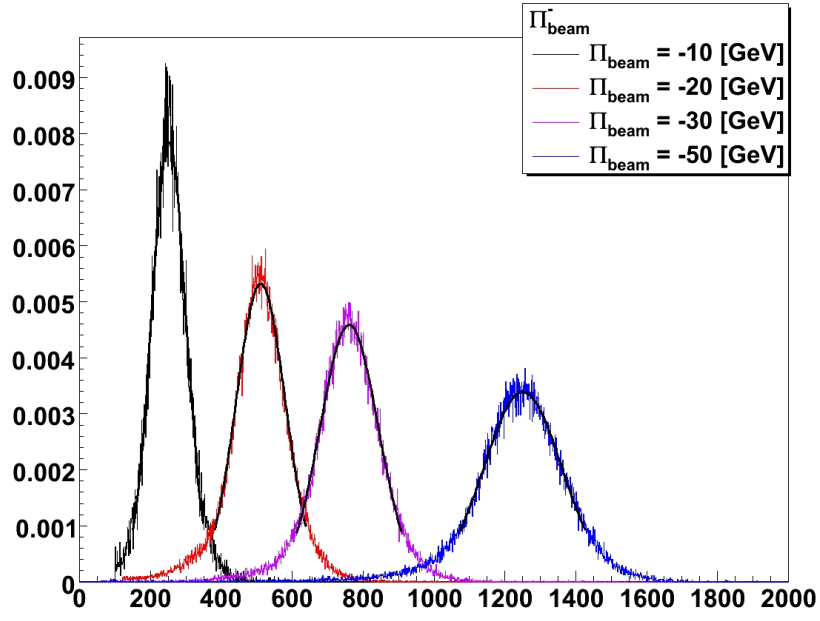


Figure 16: Energy response to π^- beam.

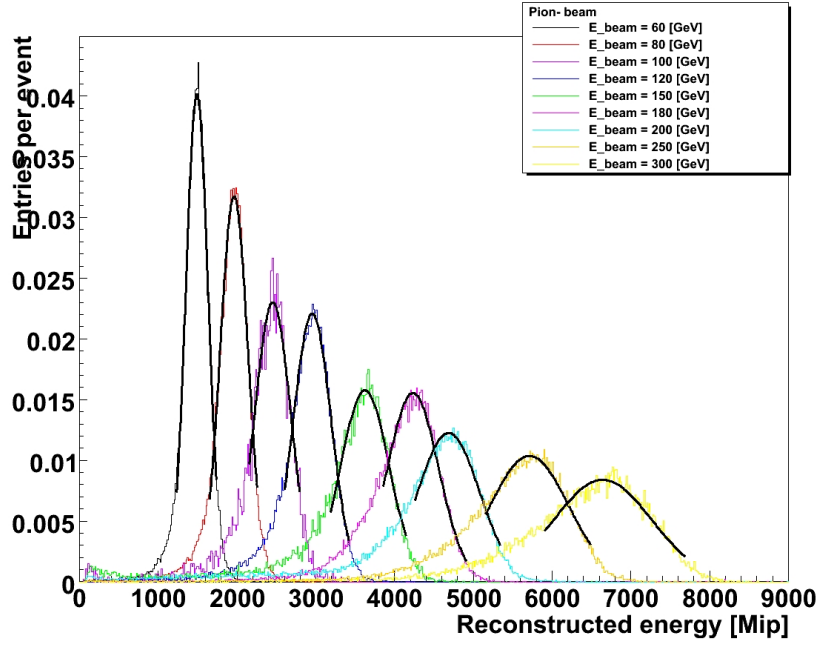


Figure 17: Energy response to π^- beam.

2.4 Linearity of response & resolution for electron beam

As can be seen on figures 13 - 17 reconstructed energy is not measured in GeV but in Mip (Minimum Ionizing Particle). Conversion from Mip to GeV is done by making a plot of obtained Mip value E_{reco} (mean value of gaussian fit to reconstructed energy distribution) as a function of available energy $E_{av} = \sqrt{p_{beam}^2 + m_{particle}^2}$. In ideal case all points would lay precisely on fit's line, but in reality this never happens. When best linear fit is obtained conversion from Mip to GeV can occur (value in Mip is divided by slope coefficient of fit) and then plot of $E_{reco}(E_{av})[GeV]$ can be obtained, from which linearity of response can be clearly seen. Such plot for electron beam is presented in figure 18. This plot contains both points from real data and point obtained from Monte Carlo generation (used models are named one plot's legend). Upper part of plot shows described linearity, lower part shows how much actual value of E_{reco} differs from it's ideal value (equal to E_{av}).

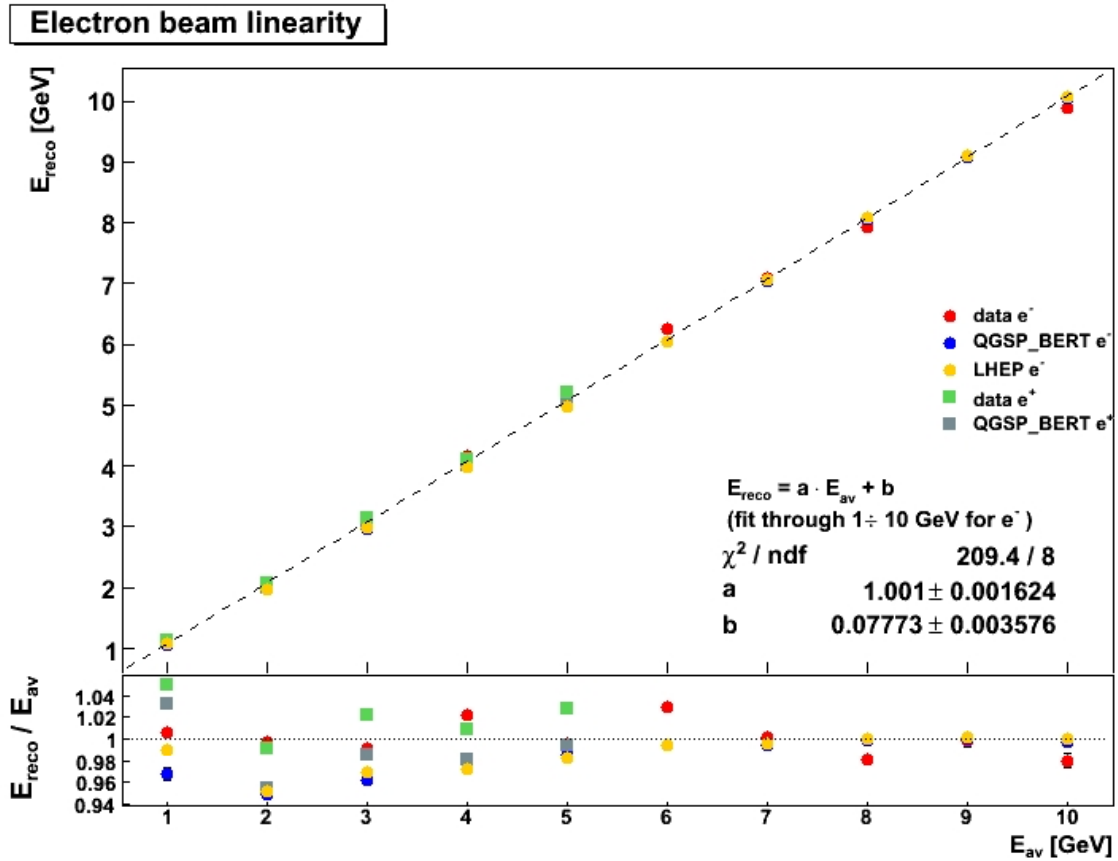


Figure 18: Linearity of response to e^\pm beam.

There are some things worth noting about plot shown above:

- positron data is shown only from 1GeV to 5GeV - reason for that is too low statistics for runs with higher energy, making them too unreliable
- electron data is shown from 1GeV to 10GeV - although higher energy runs were analysed it turned out that calibration constant for them is not ready (electron runs with energy equal and lower then 10GeV were done in 2010, with higher energies in 2011), so values obtained from them could not be trusted
- Monte Carlo generated data is in disagreement with data obtained at test beam facility

Plot shown in figure 19 shows resolution for electron beam. By resolution ratio of RMS of reconstructed energy distribution σ_{reco} to mean value of this distribution E_{reco} . Equation used to fit data points is a result of theoretical calculations and by looking at value of χ^2 (for ideal fit it should be equal to ndf) it can be seen that used fit quite nicely describes data.

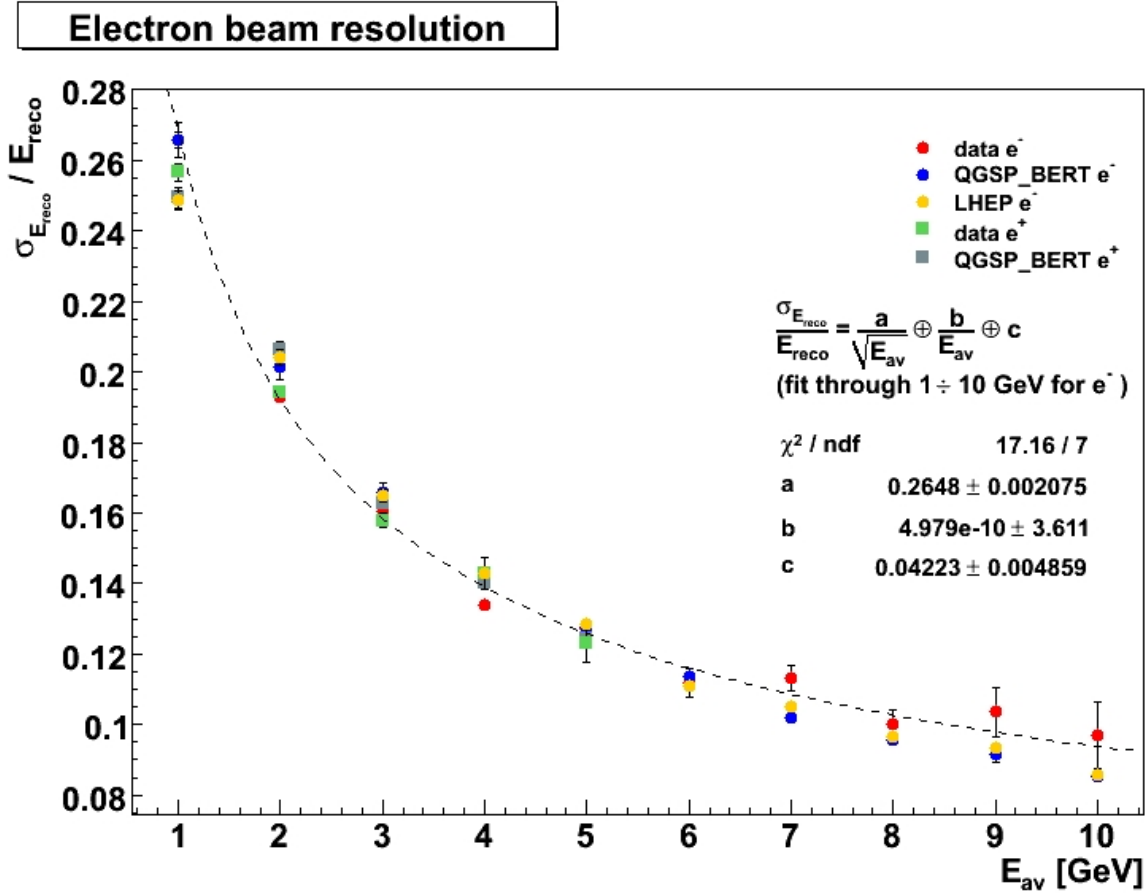


Figure 19: Resolution for e^\pm beam.

2.5 Linearity of response & resolution for pion beam

Pion runs analysis is done exactly the same way as electron run.

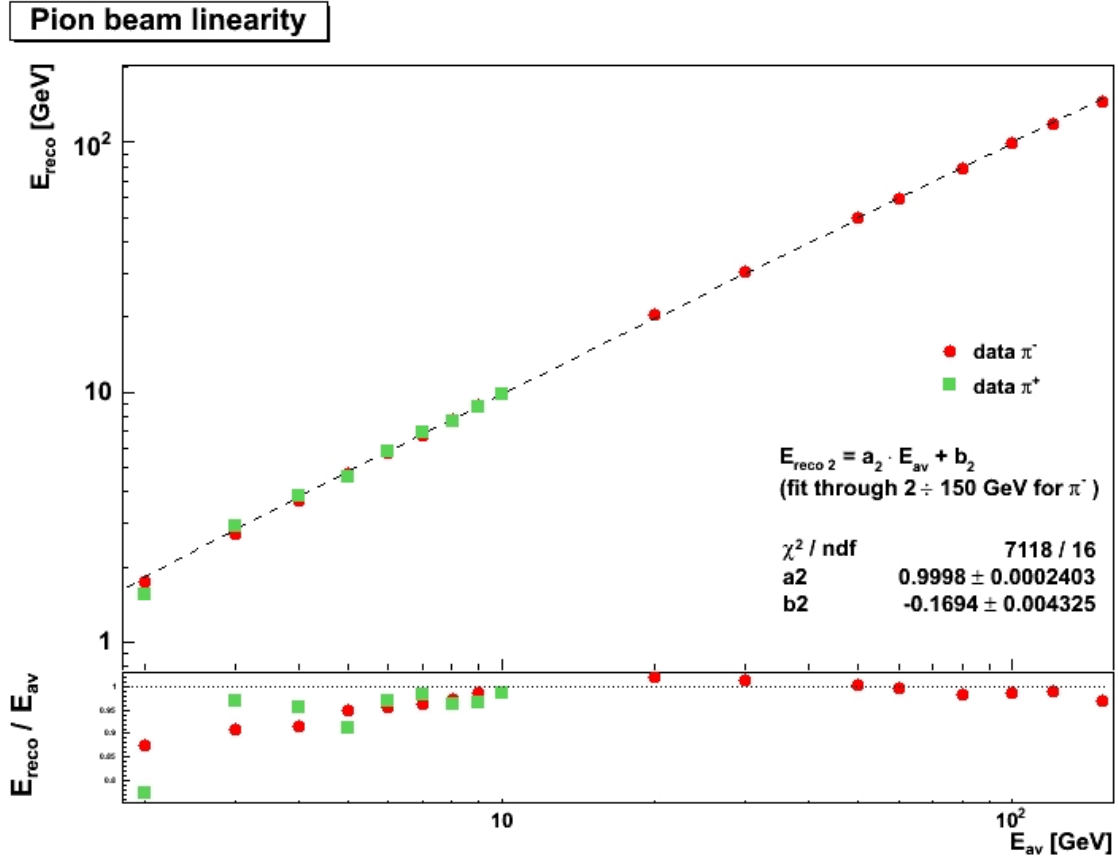


Figure 20: Linearity of response to π^\pm beam.

Things worth noting about plot shown above:

- data fit is not very good - this is a result of fact that runs with energy below 60GeV were taken in 2010 and higher energy runs in 2011 (as for electrons, calibration constant is not ready, but its value should not differ from old one); because of that this plot can be seen as preview of final results
- there are no points from Monte Carlo simulation - reason for that is unfinished computer model of prototype for 2011 runs

Figure 21 shows resolution for pion beam. It can be seen that fit is quite bad, but this might be result of lack of final calibration constant.

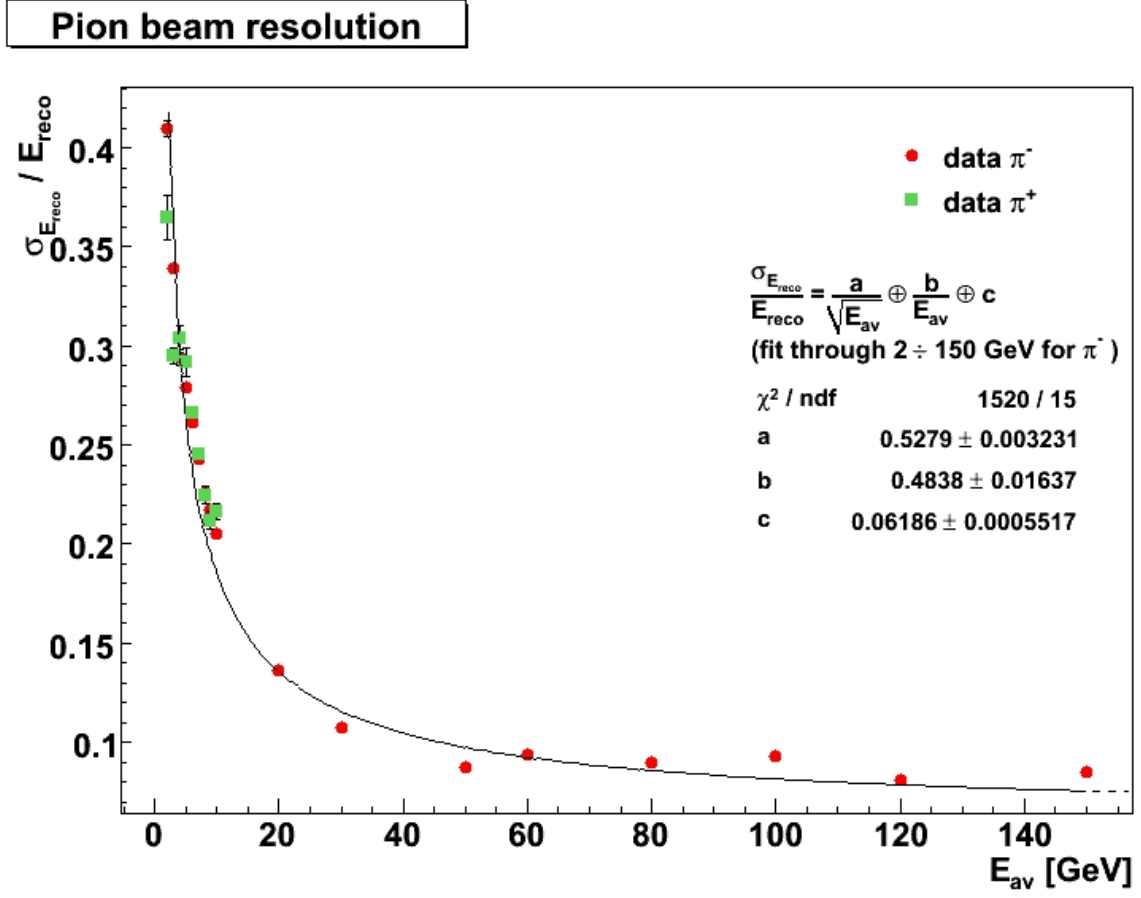


Figure 21: Resolution for $\pi^\pm beam$.

From electron and pion data plot shown in figure 22 has been obtained. It presents values of $\frac{\pi^-}{e^-}$, which were obtained by finding conversion coefficient from *Mip* to *GeV* from electron runs and then applying this coefficient to make conversion for pions. Points obtained in this way are then related to idealised electron runs (ideally linear ones) by dividing $E_{reco,\pi}$ by $E_{reco,e}$. Results are quite surprising - for tungsten this ratio was expected to be 1. Reasons for this are still unclear.

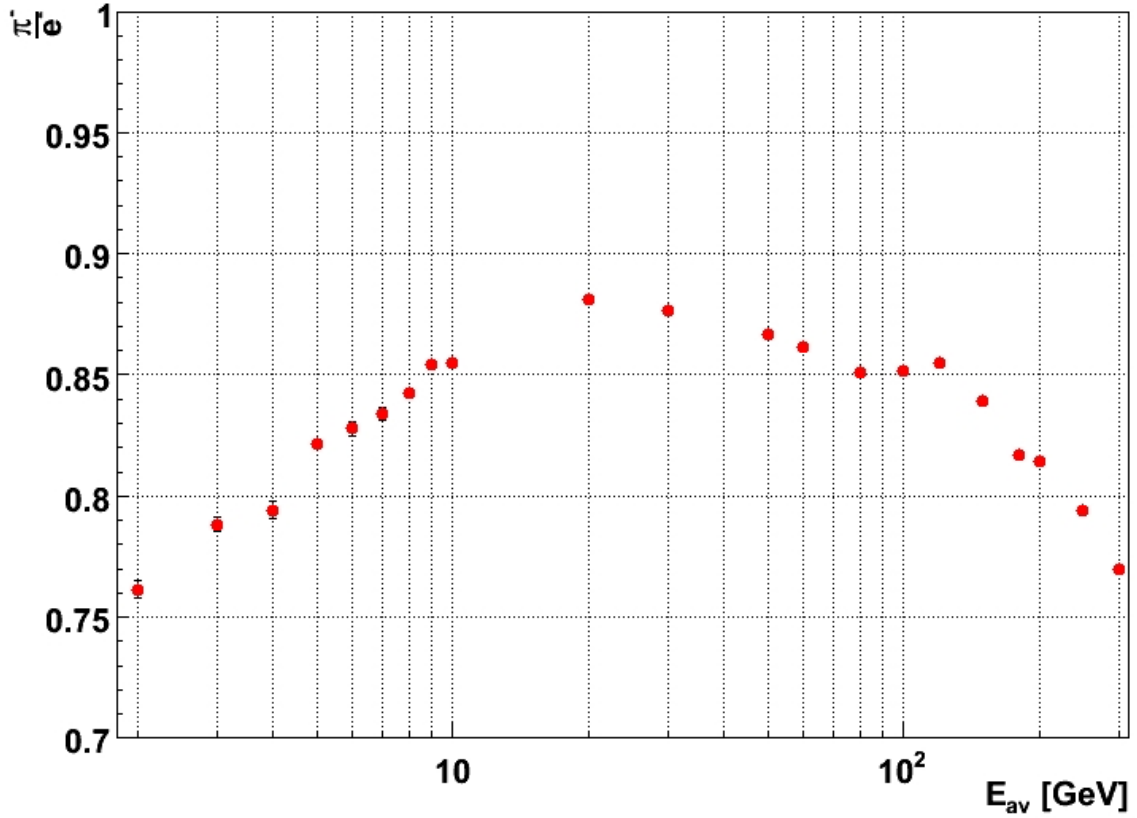


Figure 22: $\frac{\pi^-}{e^-}$ values in function of beam energy.

2.6 Temperature influence on work of detector's prototype

Influence of temperature on work of HCAL prototype has been analysed in two aspects:

- influence of temperature on value of reconstructed energy
- temperature profile of prototype

2.6.1 Influence of temperature on value of reconstructed energy

Runs with the same beam energy but taken in different temperatures were analysed and results (mean values of obtained energy distributions) were put on plot in figure 23

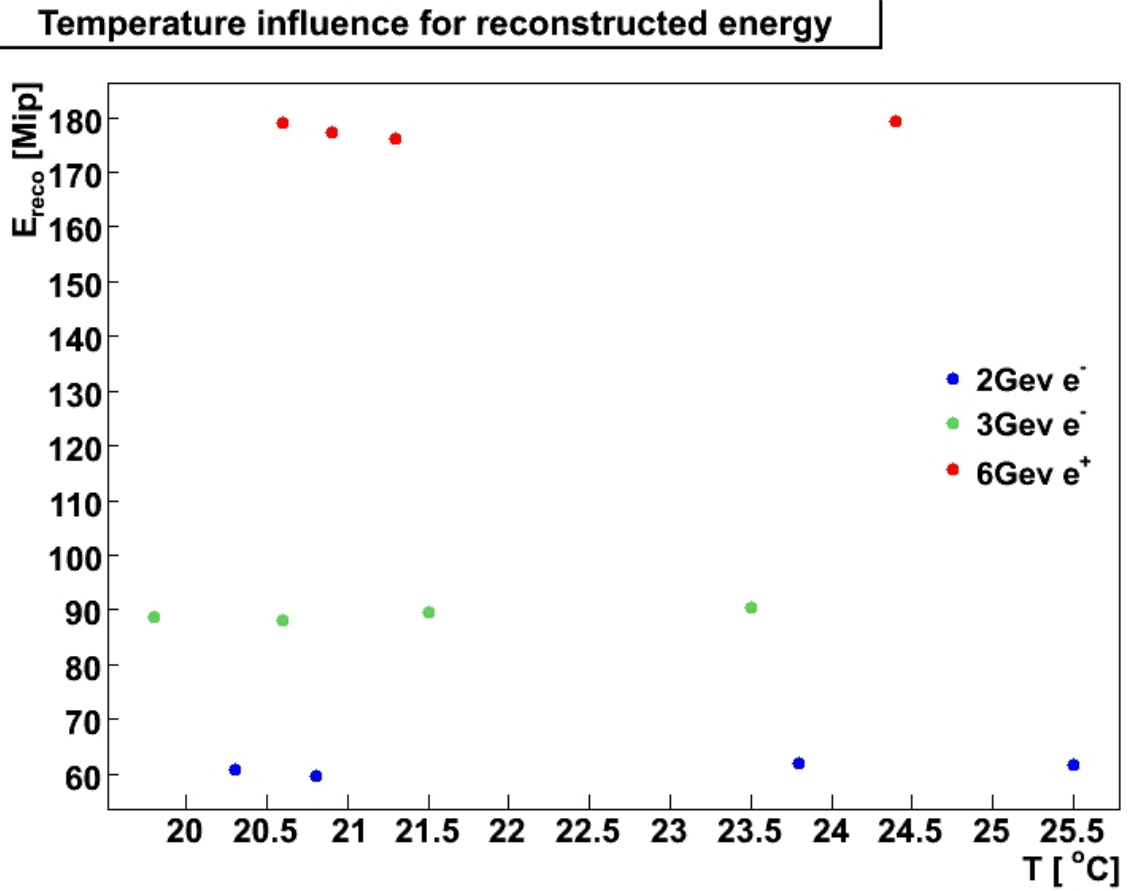


Figure 23: Mean values of reconstructed energy distribution for different runs and temperatures

Although there are not many data point available (most runs are done in similar temperatures) from plot above no temperature influence can be observed. This does not mean that detector's prototype is not sensitive to temperature (e.g. all semiconductors used to build physical prototype are in some way sensitive to temperature), but it shows that software making correction works properly.

2.6.2 Temperature profile

Physical prototype has five temperature sensors mounted on each layer. Readings from this sensors should provide temperature profile of device but it can happen that some of them do not work properly. To correct for this all sensors are calibrated with individualised constants and in case of readings outside "sanity range" (range of temperature

considered plausible to be measured in given conditions) or high difference of reading in comparison to neighbouring layers correction is applied. This correction is made by discarding faulty reading and instead of it average of neighbouring layers is computed and taken as reading.

Figure 24 shows raw temperature readings. Some spikes are observed and since such behaviour is not expected by physics they must be corrected. Left part of figure 25 shows how temperature profile looks like, when just calibration constants are applied - very big spikes (around 10000) are observed. They origin is not clear, but one possibility is that those three sensors were known to be faulty and they were marked in such way. Plot on right side of figure 25 also shows temperature profile after application of calibration constants, but not whole graph but only lower part. It can be seen that temperature profile curve is now much smoother. Final profile is shown in figure 26 - profile's curve is now sooth, there are no sudden spikes so it can be assumed that used procedure works properly.

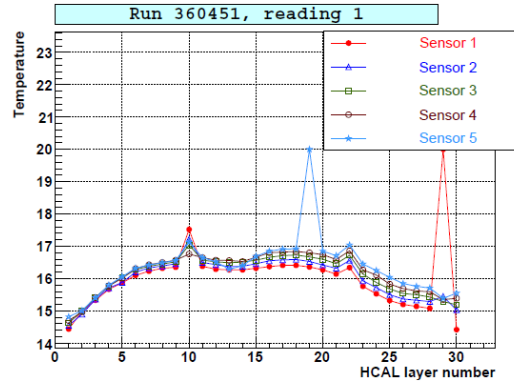


Figure 24: Raw temperature profile for 4GeV (without any calibration or correction)

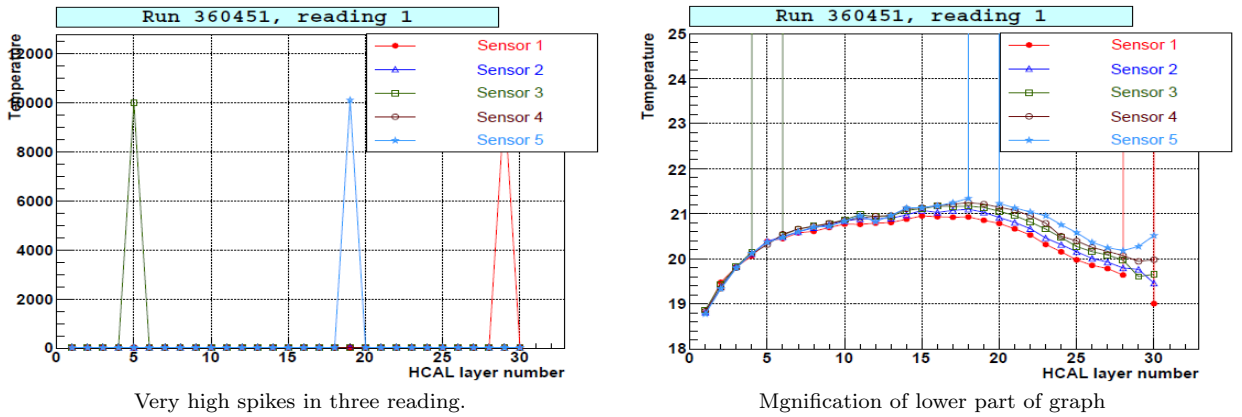


Figure 25: Temperature profile for 4GeV with calibration, without correction

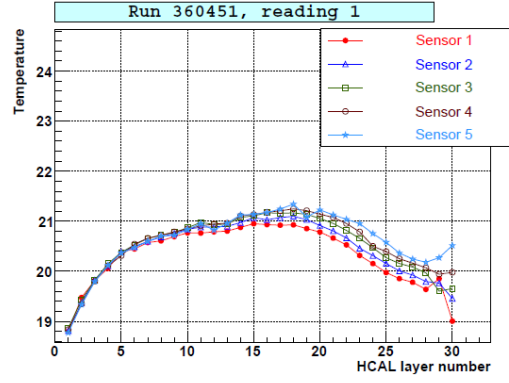


Figure 26: Final temperature profile for 4GeV (with calibration and correction)

3 Summary

Analysis of data obtained from tests of physical prototype allowed to find out how HCAL prototype behaves. It turns out that response to electron beams is quite good (linear), but for high energy pions energy leakage occurs. This problem could be resolved by adding so called Tail Catcher (detector with lower granularity, which is supposed to contain all showers escaping from HCAL). Besides problem with leakage, response to pions seems correct but 2011 calibration constant is needed to draw final conclusions. Temperature correction software works correctly, both in case of temperature influence on reconstructed energy value and temperature profile of physical prototype.

References

- [1] Commissioning of an LED Calibration & Monitoring System for the Prototype of a Hadronic Calorimeter *Nanda Wattimena*
- [2] Calorimetry at the International Linear Collider: From Simulation to Reality *Nanda Wattimena*